JOURNAL OF MATERIALS SCIENCE 31 (1996) 6463–6468

Single-crystal $K_x(Zn_yTi_{8-y})O_{16}$ priderites: growth and characterization

A. K. BHATTACHARYA, R. G. BISWAS, K. K. MALLICK
Centre for Catalytic Systems and Materials Engineering, Department of Engineering, University of Warwick, Coventry CV4 7AL, UK

Single crystals of $K_x(Zn_yTi_{8-y})O_{16}$ priderites have been grown from a melt of K_2O–MoO_3 using the flux-zone technique. High-purity crystals > 10 mm in length were obtained, with no indication of twinning. Lattice parameters of $a = 1.0162(8)$ nm and $c = 0.2971(7)$ nm were obtained from X-ray diffraction measurements. Habit planes were identified from scanning electron microscope images. X-ray photoelectron spectroscopy confirmed the titanium oxidation state as +4. High-temperature complex impedance spectroscopy between 300 and 820 K was used to electrically characterize the crystals. This indicated that the materials had a low d.c. conductivity and a conductivity of 1.68×10^{-3} S cm^{-1} at 100 kHz.

1. Introduction

Alkali-doped titanates with the general formula $A_x(B_yTi_{8-y})O_{16}$ where A is an alkali or alkaline-earth metal or barium, and B is a di- or tri-valent cation, are known as priderites. They are isostructurally similar to the mineral "hollandite" and are known as one-dimensional ionic conductors due to the tunnel structures formed by the ionic framework of double rutile-like chains of (B, Ti)O_6 octehedra [1]. Substitution of Ti^{4+} by B^{2+} ions places a negative charge on the framework that is compensated by large alkali or alkaline-earth A cations in the tunnel channel. The size of the framework is then dependent on the ionic radius of substituting B element. The A ions are the mobile species and are situated in non-communicating tunnels. These tunnel structures have also been investigated as one-dimensional superionic conductors, where K^+ tunnel ions are found to give the highest conductivity. Hollandite structures, as a constituent of SYNROC, are also investigated as Cs^+ immobilizers in nuclear waste disposal applications [2].

Tunnel structures are an interesting system in which to study one-dimensional conduction properties as the conductivity can be varied by the substitution of dopant ions whose size is comparable to the tunnel channels. Also, mobile ions are influenced by potential barriers which is unlike two- or three-dimensional systems where the mobile ions can move around such barriers. The conduction properties have been theoretically investigated by Beyler [3] and Bernasconi [4]. Experimental conductivity studies, mainly at low temperature, have been carried out on K^+, Rb^+, Li^+ and Cs^+ as the tunnel ion, and Mg^{2+}, Zn^{2+} and Al^{3+} for the octahedral cation [5–8]. In K^+ priderite, the conductivity has been found to be sensitive to the effects of potential barriers produced by crystal defects [6], disorder produced by the mobile ions [9], the size of the ionic framework [10], and the dopant ion size [5, 9].

Complex impedance spectroscopy techniques have been used to measure the electrical conductivity properties of K_x (Zn, Mg)$_{x/2}Ti_{8-x/2}O_{16}$ solid solutions [8] and more recently on single crystals of Ba–Al and K–Zn priderites [6, 7]. Previous work on pelleted solid solutions [8] though may not have given a true indication of the bulk conductivity due to the highly anisotropic nature of the conduction process in one-dimensional priderites. Measurements have been shown to be difficult due to the high d.c. resistance of the samples and the difficulty in removing the contribution of the electrode.

In this paper we give details on the growth of $K_x(Zn_yTi_{8-y})O_{16}$ priderite single crystals by the flux-zone method. The crystals have been characterized to determine the habit planes, lattice parameters, composition, surface state and electrical conductivity.

2. Experimental procedure

The K–Zn priderites were grown using the flux-zone method. Starting materials for the crystal growth were K_2CO_3 powders of 99.99% purity, and TiO_2 and ZnO powders of 99.999% purity. The growth of single crystals was carried out by the slow cooling technique of the flux method. Typical fluxes employed were based on the K_2O–MoO_3 system, which can be considered to be a K_2O–MoO_3 mixture with MoO_3 acting as an active solvent in such a system. The addition of alkali ions reduced the vapour pressure and as result, the volatilization of MoO_3 could be significantly reduced. The optimum composition of the most successful flux that produced twin-free crystals was found to be $K_2O(MoO_3)_{1.7}$.

0022–2461

A 200 ml platinum crucible with a tightly fitting lid was used in all runs. The crucible, filled with the thoroughly mixed starting materials, was heated to 1400 °C for 12 h in a $MoSi_2$ high-temperature furnace and subsequently cooled slowly to 850 °C at a rate of 2 °C h^{-1}. The crucible was then removed from the furnace and rapidly cooled to room temperature. The grown crystals were then recovered by dissolving the flux in hot water.

Elementary and morphological analysis of the crystals was carried out in a Jeol scanning electron microscope (JEM 6100) operating at 20 kV and equipped with an energy dispersive X-ray analyser (EDX). Conducting samples were prepared by carbon coating small single crystals. Both broad-beam and point EDX analyses of powder particles were performed using manganese as a reference standard. The EDX analyses of the crystal using different spot sizes were averaged.

X-ray powder diffraction (XRD) patterns of crushed crystals were recorded in the region of $2\theta = 10°–80°$ with a scanning speed of $1/4°\ min^{-1}$ on a Philips diffractometer (Model PW1710) using CuK_α radiation with a nickel filter.

X-ray photoelectron spectroscopy (XPS) analysis was performed using a Kratos XSAM 800 on crushed crystals. MgK_α X-rays were used as the excitation source. Peak positions were corrected using the C1s peak at 284.5 eV to account for sample charging.

Electrical characterization was carried out by using the technique of complex impedance spectroscopy. Contacts were applied using Englehard 6082 platinum ink and platinum wire. The ink was painted to the ends of several different length crystals and fired at 580 °C for 2 h. Samples were mounted in a temperature-controlled furnace with a flowing argon atmosphere. Characteristics were measured using a Solartron 1260 impedance/gain-phase analyser. A 10 mV excitation signal was used and data auto-integrated over 100 s [11] to obtain data at low frequencies.

3. Results and discussion

3.1. Growth conditions

The various flux compositions and growth conditions produced varying degrees of second phases such as rutile as well as twinning, a common form of crystal imperfection. The optimum composition of the most successful flux that produced twin-free crystals was found to be $K_2O(MoO_3)_{1.7}$ resulting in crystals of maximum size (> 10 mm). A high liquidus temperature of above 1300 °C combined with a cooling rate of no less than 4 °C h^{-1} from above 900 °C, improved both the quality and size of the crystals produced.

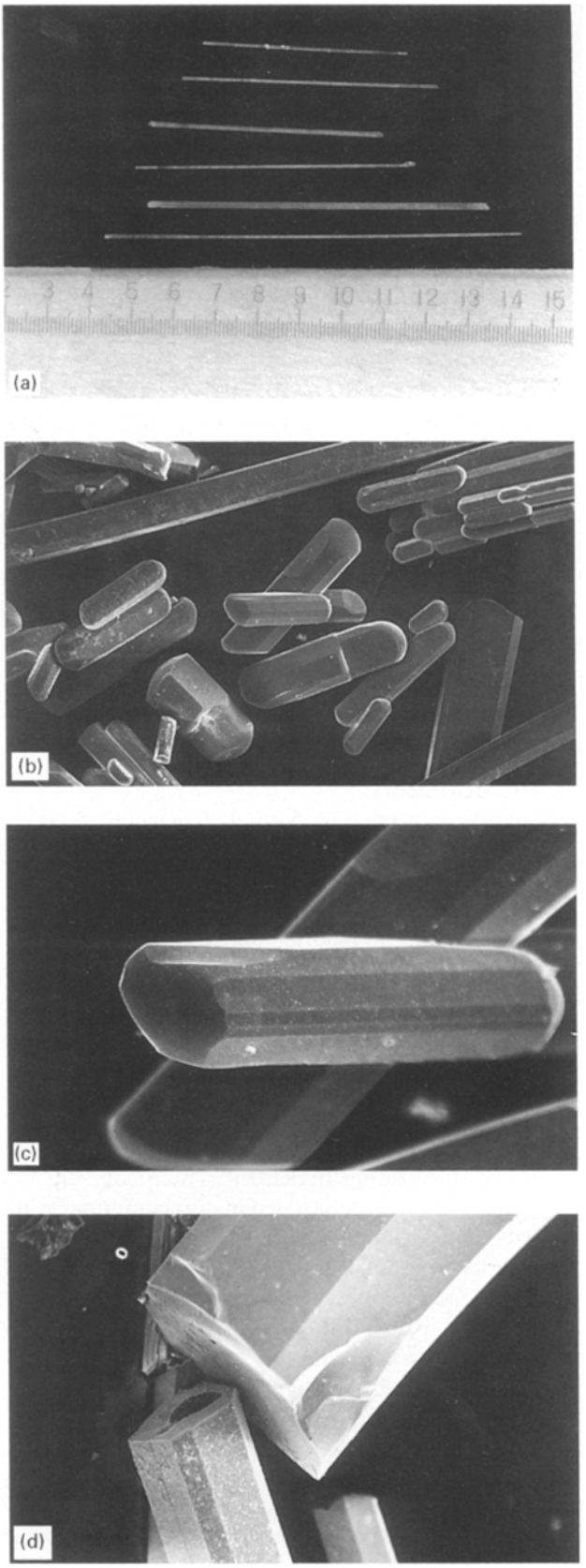

Figure 1 (a) Optical photograph of some $K_x(Zn_yTi_{8-y})O_{16}$ crystals. (b–d) SEM images of some typical K–Zn-priderite crystals, showing various sizes, habit planes, and pyramidal facets.

3.2. Crystal habit

Transparent crystals of K-priderites, > 10 mm long, as shown in Fig. 1a, were successfully grown with no evidence of twinning, usually associated with the growth of such crystals. The crystals were found to have a very slight yellowish hue. The growth of crystals occurred in an acicular form elongated along the *c*-axis. The SEM study of some crystals, Fig. 1b–d, showed examples of the typical morphology and habit of the crystals. Crystal habit was assigned to the family of {1 0 0}, {1 1 0}, {2 2 0} and {3 3 0} planes and a typical selection of the prismatic faces is shown

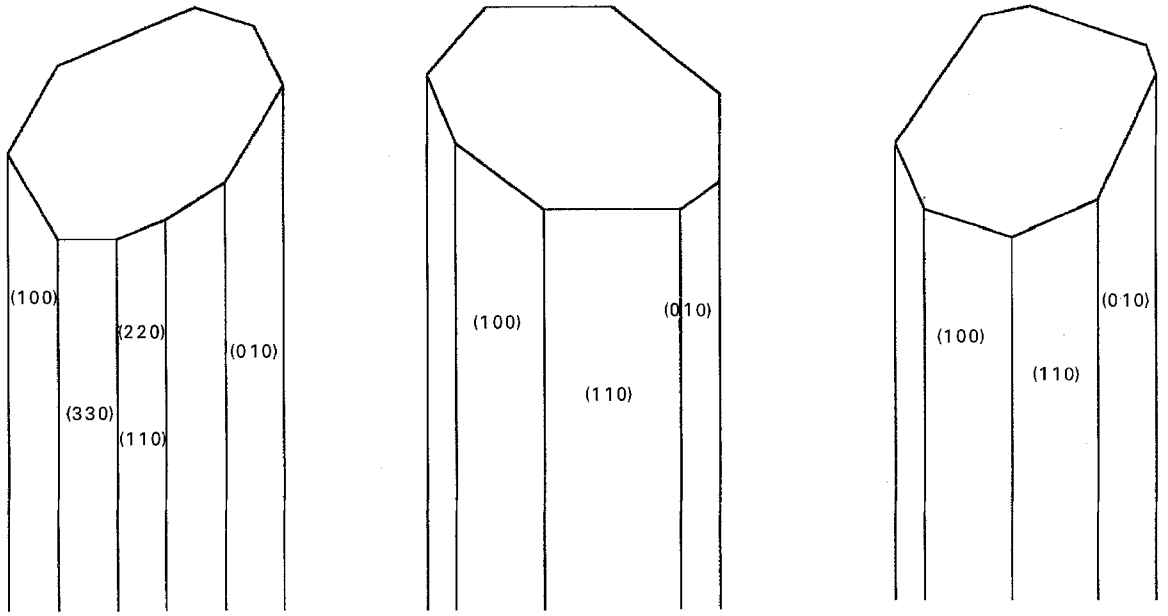

Figure 2 Typical identified habit planes of our crystals.

schematically in Fig. 2. Where smooth pyramidal faces are seen, the crystals were long and the terminal faces were sometimes hollowed, as seen in Fig. 1d.

3.3. Composition

The SEM–EDX point analysis of the composition of individual single crystals is given in Table I. The results conformed to the general formula $A_x(B_yTi_{8-y})O_{16}$ where A ions are normally in the range $x = 1.55$–1.67. In the present case, y for zinc as the B-ion ranges between 0.8 and 0.9. Because the value of y is independent of the type of the B-element substituting for Ti^{4+}, the change of x seen here indicates that K^+ as the A-ion is easily mobile in the tunnel having one vacancy on four sites. The actual concentration of the potassium incorporated into the crystal during growth may also have been influenced by an impurity such as sodium which acts as an impurity barrier for conductive motion of the K^+ ion.

There are detectable differences in composition and this is probably related to the habit change observed in these crystals. Although high-purity fluxes were employed, the partial substitution of any residual impurities such as sodium or other alkaline metals cannot be ruled out. However, in this case, the level would be at the parts per million level and is not therefore expected to affect the conductivity values.

TABLE I Composition determined by SEM-EDX

System	Composition
$K_xZn_yTi_{8-y}O_{16}$	$K_{1.55}Zn_{0.90}Ti_{7.10}O_{16}$
$0.8 < y < 0.9$	$K_{1.57}Zn_{0.84}Ti_{7.16}O_{16}$
	$K_{1.58}Zn_{0.82}Ti_{7.18}O_{16}$
	$K_{1.67}Zn_{0.80}Ti_{7.20}O_{16}$

3.4. Surface analysis

The Ti 2p peak positions, shown in Fig. 3, were observed at $Ti\,2p^{3/2} = 458.5$ eV and $Ti\,2p^{1/2} = 464.3$ eV giving a separation of 5.8 eV. Literature values for TiO_2 are $Ti\,2p^{3/2} = 458.5$ eV and a separation of 5.7 eV. Apart from small experimental errors the analysis of the priderite is nearly identical to that of TiO_2 which suggests that the titanium oxidation state is +4 and further that the chemical environment of the titanium atoms is similar to the oxide.

3.5. Cell dimensions

Typical lattice constants and other cell parameters for K-priderite crystals are summarized in Table II. They

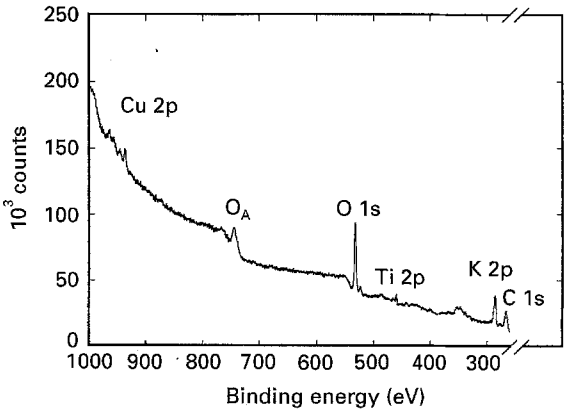

Figure 3 Binding energy plot of K–Zn-priderite crystals.

TABLE II Lattice parameters of $K_x(Zn_yTi_{8-y})O_{16}$

	a (nm)	c (nm)	$V(10^{-3})$ nm^3
$K_{1.67}Zn_{0.80}Ti_{7.20}O_{16}$[a]	1.016 2(8)	0.297 1(7)	306.92
$K_{1.56}Zn_{0.76}Ti_{7.24}O_{16}$[4]	1.016 1(4)	0.297 3(4)	307.11

[a] Present work.

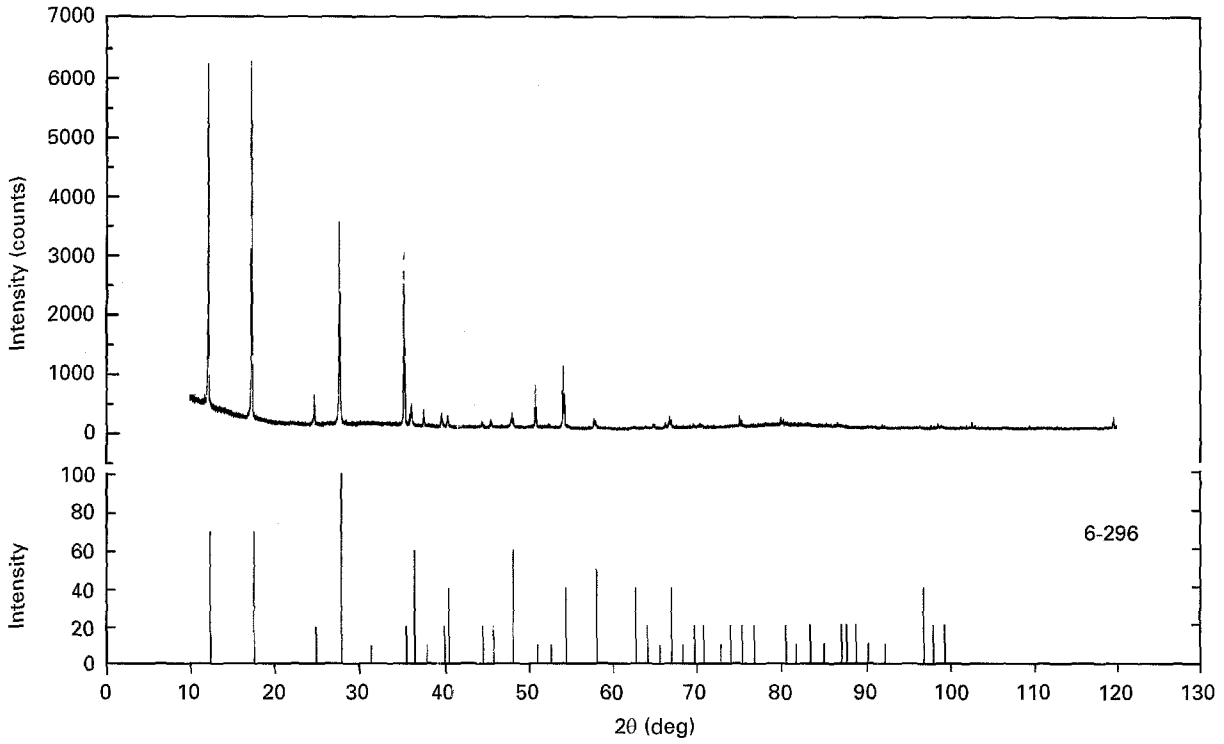

Figure 4 XRD pattern of K–Zn-priderite crystal compared to published JCPDS data for (K, Ba) $(Ti, Fe)_8O_{16}$.

were calculated and refined using Philips APD 1700 programme from X-ray diffraction data based on the space group *I*4/*m*. The X-ray diffractogram shown in Fig. 4 matches reasonably well with the published JCPDS data for (K, Ba) $(Ti, Fe)_8O_{16}$ and lattice parameter values agree well with those published for comparable compositions for K–Zn-priderites [6].

3.6. Impedance spectroscopy

Measurements of the complex admittance (Y^*), obtained from complex impedance measurements, can be separated into real and imaginary components using the relation of $Y^*(\omega) = Y'(\omega) + jY''(\omega) = [\sigma_a(\omega) + j\omega\varepsilon_0\varepsilon'(\omega)]$, where ω is the angular frequency, ε' is the permittivity and $\sigma_a(\omega)$ the frequency-dependent

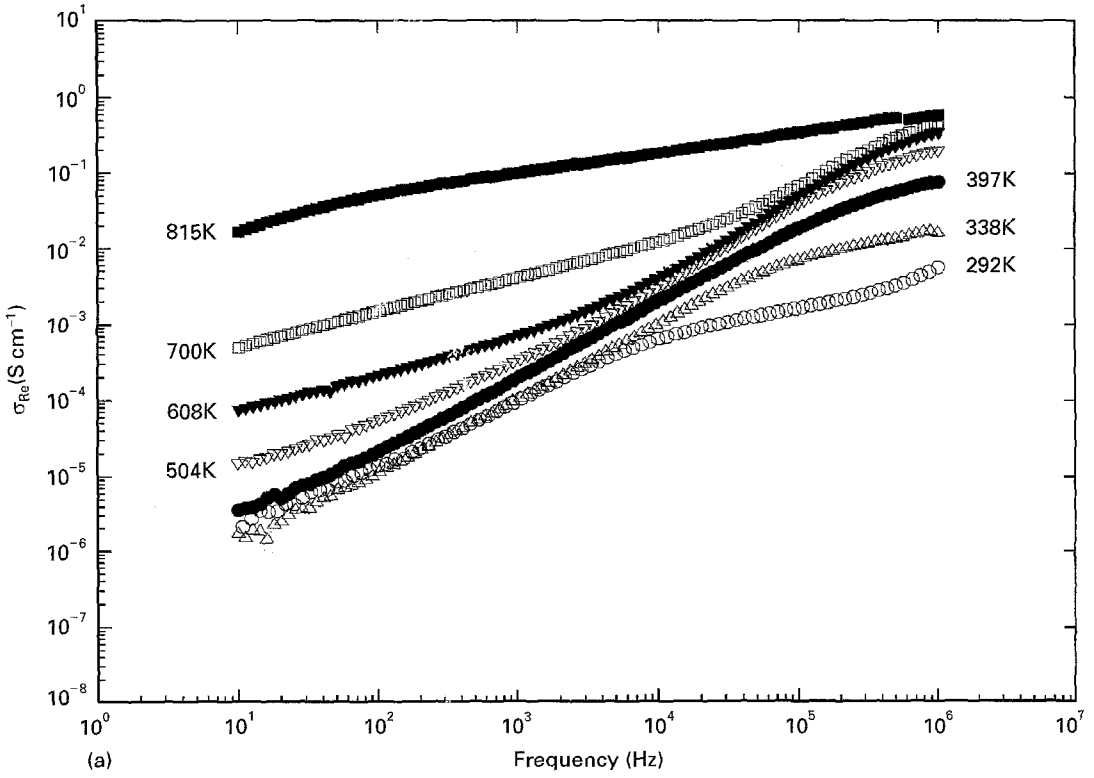

Figure 5 Frequency dependence of the (a) real part of the total conductivity, (b) imaginary part of the total conductivity of K–Zn-priderite.

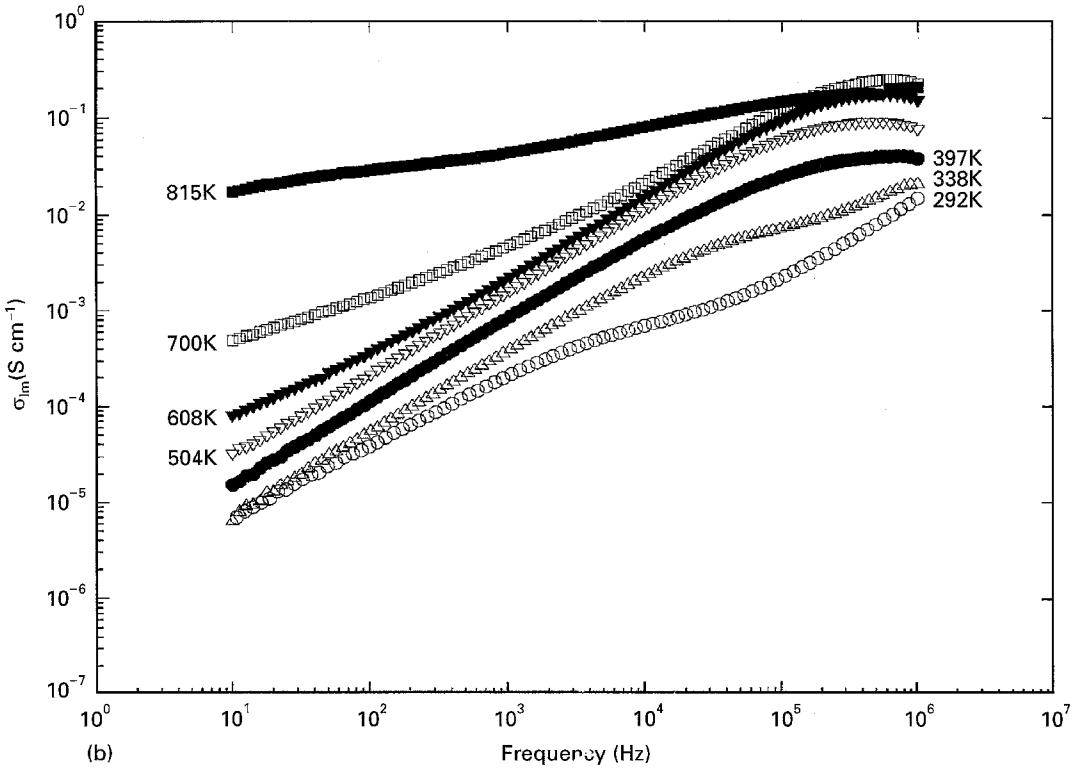

Figure 5 Continued.

conductivity. The real and imaginary parts of the total conductivity from one of our K–Zn-priderite crystals is given in Fig. 5a, b. The data shown, are for various isotherms where the measurement frequency was swept between 10 Hz and 1 MHz. The power-law dependence of the conductivity of $\sigma(\omega) \propto (j\omega)^{v}$ as proposed by Bernasconi *et al.* [4], can be seen in the data at 292 K above 10^4 kHz. Other crystals measured showed similar characteristics. The curves display similar characteristics to those of other priderites [10] and have a conductivity of 1.68×10^{-3} S cm^{-1} at 100 kHz.

The conductivity at high frequency saturates for each isotherm, indicating a thermal activation of the mobile ion. The graphs also indicate that the crystals have a high d.c. resistance and that the electrode contributes significantly to the overall conductance spectrum up to a frequency of 10^4 kHz. This is further shown by a Nyquist plot, Fig. 6, at 292 K, where a single semicircle indicative of a single crystal and an electrode contribution occurring at an angle of 75°, as compared to a theoretical 90° for blocking contacts, are found.

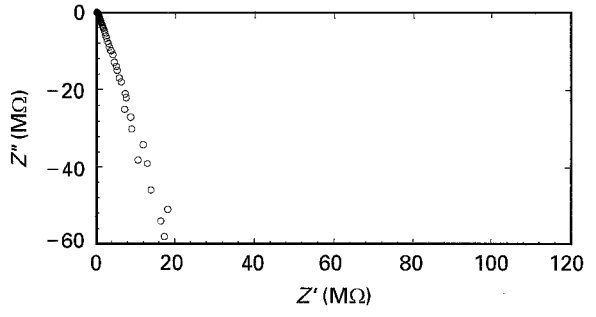

Figure 6 Nyquist plot of K–Zn-priderite at 292 K.

4. Conclusion

High-quality single crystals of K–Zn-priderite have been grown using the flux-zone method. The most successful flux was found to be $K_2O(MoO_3)_{1.7}$. The crystals were characterized by XRD, SEM, EDAX, XPS and impedance spectroscopy. The crystals showed no evidence of twinning and typical habit planes were identified. Lattice parameters of $a = 1.016\,2(8)$ nm and $c = 0.297\,1(7)$ nm were obtained. XPS confirmed the Ti^{4+} oxidation state. High-temperature conductivity studies were performed which showed thermal activation of the K^+ ion and a power-law dependence $\sigma(\omega) \propto (j\omega)^{v}$ as predicted by theory. A conductivity of 1.68×10^{-3} S cm^{-1} at 100 kHz was found.

Future work will include growth of doped crystals and measurements of the conductivity over a wider temperature range to obtain activation energies and to observe dependencies on the framework size and mobile ion radius.

References

1. M. WATANABE, Y. FUJIKI, Y. KANAZAWA and K. TSUKIMURA, *J. Solid State Chem.* **66** (1987) 56.
2. R. W. CHEARY, *Acta Crystallogr.* **B47** (1991) 325.
3. H. U. BEYELER and S. STRASSLER, *Phys. Rev. B* **24** (1981) 2121.
4. J. BERNASCONI, H. U. BEYLER, S. STRASSLER and S. ALEXANDER, *ibid.* **42** (1979) 819.

5. S. YOSHIKADO, T. OHACHI, I. TANIGUCHI, Y. ONADA, M. WATANABE and Y. FUJIKI, *Solid State Ionics* **7** (1986) 335.
6. Y. KUDOH, H. BANNAI, S. YOSHIKADO, Y. ONADA and Y. FUJIKI, *J. Ceram. Soc. J.* **96** (1988) 98.
7. S. YOSHIKADO, T. OHACHI, I. TANIGUCHI, Y. ONADA, M. WATANABE and Y. FUJIKI, *Solid State Ionics* **18–19** (1986) 507.
8. J-M. REAU, J. MOALI and P. HAGENMULLER, *J. Phys. Chem. Solids* **38** (1977) 1395.
9. H. U. BEYELER, L. PIETRONERO and S. STRASSLER, *Phys. Rev. B* **22** (1980) 2988.
10. S. YOSHIKADO, T. OHACHI, I. TANIGUCHI, Y. ONADA, M. WATANABE and Y. FUJIKI, *Solid State Ionics* **7** (1986) 335.
11. Solartron Application Note MAN/CWB/0693.

Received 23 October
and accepted 20 November 1995